

Carving complex many-atom entangled states by single-photon detection

Wenlan Chen, Jiazhong Hu, Yiheng Duan, Boris Braverman, Hao Zhang, and Vladan Vuletić
*Department of Physics and Research Laboratory of Electronics,
 Massachusetts Institute of Technology, Cambridge, Massachusetts 02139, USA*

We propose a versatile and efficient method to generate a broad class of complex entangled states of many atoms via the detection of a single photon. For an atomic ensemble contained in a strongly coupled optical cavity illuminated by weak single- or multi-frequency light, the atom-light interaction entangles the frequency spectrum of a transmitted photon with the collective spin of the atomic ensemble. Simple time-resolved detection of the transmitted photon then projects the atomic ensemble into a desired pure entangled state. Complex entangled states such as multicomponent Schrödinger cat states can be generated with high fidelity. This probabilistic but fast heralded state-carving method can be made quasi-deterministic by repeated trial and feedback, yields high success probability per trial, and can be implemented with existing technology.

PACS numbers: 03.67.Bg, 32.80.Qk, 42.50.Dv, 42.50.Pq

Entanglement is a useful resource in physics. By means of interatomic entanglement, it is possible to overcome the standard quantum limit associated with projection noise in atom interferometers and atomic clocks [1–11]. Entanglement can also be used to implement secure communication networks [12–14] that are protected by fundamental principles of quantum physics. Furthermore, entanglement may enable more efficient computation algorithms, potentially with significant impact on computer science [15–19].

Entanglement in many-particle systems is non-trivial to generate, and often as challenging to experimentally verify. Entanglement implies correlations between the particles, and hence its generation requires controlled interactions between many particles. Therefore, the difficulty of generating entanglement typically dramatically increases both with particle number, and with the complexity of the entangled state. Most entangled states of many atoms generated so far have been relatively simple, characterized by positive Gaussian quasi-probability distribution functions (spin squeezed states) [3–11, 20], or a Wigner function with at most one negative region [21]. More complex entangled states [22], Greenberger-Horne-Zeilinger states [23], have been generated in chains containing up to 14 ions by means of the Coulomb interaction [24–26].

The generation of a desired entangled state requires the controlled application of one or more specific many-body interaction Hamiltonians. Even when a suitable interaction between many particles can be implemented, it is in general difficult to realize pure atomic states, as entanglement with unobserved degrees of freedom leads to decoherence and loss of fidelity in the variables of interest. Thus, with the exception of Ref. [21], all entangled states of many atoms generated to date have been mixed quantum states with low purity. In the work by McConnell et al. [21], a scheme to generate entanglement in many-atom ensembles by probabilistic photon detection is used [27–29], where probability of entanglement generation is

traded in for high state purity on rare but heralded occasions [12]. However, for that method the success probability decreases exponentially for more complex states with smaller structures in the Wigner function [27].

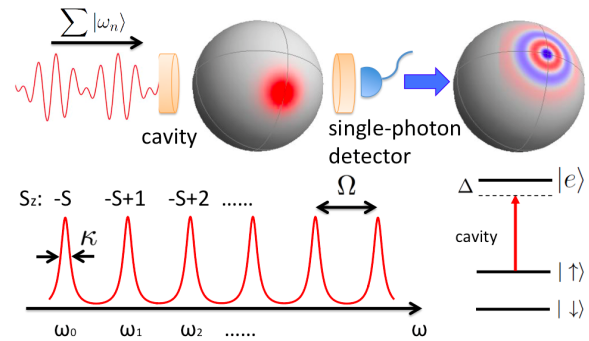


FIG. 1. Setup for entangled-state generation in atomic ensembles by single-photon detection. The cavity mode couples one of the ground states $|\uparrow\rangle$ to an electronic excited state $|e\rangle$ with a detuning Δ . The system operates in the strong-coupling regime (cooperativity $\eta \gg 1$), such that each atom in $|\uparrow\rangle$ shifts the cavity resonance by an amount $\Omega > \kappa$, where κ is the cavity linewidth. We first prepare all N atoms in $|\downarrow\rangle$ and rotate the collective atomic spin by an angle θ . Then, we send in a weak optical pulse $\sum |\omega_i\rangle$ containing multiple frequency components that coincide with possible cavity resonance frequencies. Once the photon detector registers a transmitted photon, the atomic ensemble is projected into a known entangled state, that is determined by the spectrum of the incoming light and the detection time of the photon.

In this Letter, we propose a heralded scheme to universally engineer a broad class of complex entangled states simply by the detection of one photon. When a strongly coupled ensemble-cavity system [30] is illuminated by a weak light field, the atom-light interaction entangles every eigenstate of the collective atomic spin (Dicke state [31]) with a corresponding frequency component of a photon transmitted through the cavity. A coherent superposition of different Dicke states with arbitrary amplitudes

and phases can be engineered by spectral shaping of the input photon, recording a transmitted photon, and rotating the atomic spin conditioned on the detection time of the transmitted photon. This represents a powerful technique to "carve" a complex entangled state out of an unentangled product state of the individual atomic spins via the detection of just one photon. The proposed method is efficient in that the generation probability is simply given by the overlap of the initial unentangled state with the target state. The accessible states, that include individual Dicke states [32], squeezed Schrödinger cat states, and maximally entangled GHZ-like states [23], can have small features in phase space, and correspondingly large Fisher information [33], thus enabling atomic clocks and interferometers operating beyond the standard quantum limit [27].

We consider N three-level atoms trapped inside, and uniformly coupled to, an optical cavity (Fig. 1). Two ground states, labeled $|\uparrow\rangle$ and $|\downarrow\rangle$, correspond to a pseudospin \vec{s}_i of atom i with $s_i = 1/2$, and we define a collective spin $\vec{S} \equiv \sum \vec{s}_i$. An excited state $|e\rangle$ is coupled to one of the ground states $|\uparrow\rangle$ by the cavity mode. The detuning between the cavity mode and the atomic transition is Δ . By adiabatically eliminating the excited state, the interaction Hamiltonian can be written as [34]

$$H = \hbar\Omega(S_z + S)\hat{c}^\dagger\hat{c}. \quad (1)$$

Here, $\Omega = g^2/\Delta$ is the coupling strength, $S = N/2$ is the magnitude of the collective spin \vec{S} , $2g$ is the single-photon Rabi frequency, and for the moment we are ignoring the scattering of photons into free space by the atoms, and the associated reduction in cavity transmission. Each atom in state $|\uparrow\rangle$ shifts the cavity resonance by a frequency $\Omega \ll \Delta$. When Ω is larger than a few cavity linewidths κ , each possible value of S_z ($S_z = -S, -S+1, \dots, S-1, S$) corresponds to a resolved cavity line. We define ω_c as the cavity resonance without any atoms in $|\uparrow\rangle$, so the resonance frequency of the cavity with $n = S_z + S$ (the n -th Dicke state) atoms in state $|\uparrow\rangle$ is $\omega_n = \omega_c + n\Omega$.

We first initialize all N atoms in $|\downarrow\rangle$, i.e. $S_z = -S$, and rotate this coherent spin state (CSS) on the Bloch sphere into a direction given by the polar angle θ and the azimuthal angle ϕ :

$$|\theta, \phi\rangle = (\cos(\theta/2)|\downarrow\rangle + e^{i\phi}\sin(\theta/2)|\uparrow\rangle)^{\otimes N}. \quad (2)$$

For the following, it is convenient to write the CSS $|\theta, \phi\rangle$ in the Dicke basis $|S, S_z = -S + n\rangle$. Thus $|\theta, \phi\rangle = \sum_{n=0}^{2S} c_n |S, -S + n\rangle$ with coefficients [35]

$$c_n = \sqrt{\binom{2S}{n}} e^{in\phi} \cos^{2S-n}(\theta/2) \sin^n(\theta/2). \quad (3)$$

We prepare the incident light field by modulating a weak pulse of monochromatic light so that it acquires

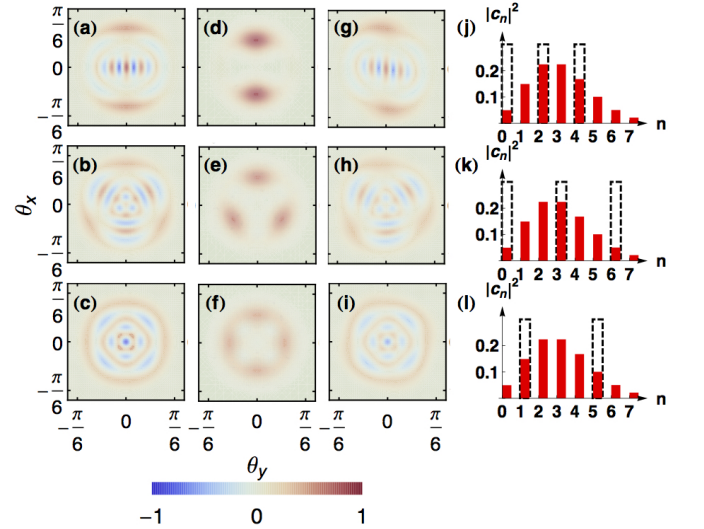


FIG. 2. Examples of two-, three- and fourfold symmetric Schrödinger cat states of collective atomic spin generated by detecting one photon. 100 atoms are initialized in a rotated CSS $|\theta, \phi\rangle$ with $\theta = 0.248$ rad and $\phi = 0$. Fig. (a)-(f) show the entangled states generated with an ideal cavity of infinite cooperativity η . (a)-(c) are the plots of the Wigner function and (d)-(f) are the plots of the Husimi Q function, $Q = 2\langle\theta, \phi|\rho|\theta, \phi\rangle$, where ρ is the atomic density matrix. Here the first row shows the superposition of Dicke states $n = 0, 2$ and 4 , the second row shows the superposition of $n = 0, 3$ and 6 , and the third row shows the superposition of $n = 1$ and 5 . We also plot the Wigner function for the non-ideal case in Fig. (g)-(i). Here, we use realistic parameters for the cavity cooperativity $\eta = 200$, detuning $\Delta = 2\pi \times 66$ MHz, atomic excited state decay rate $\Gamma = 2\pi \times 5.2$ MHz, and cavity linewidth $\kappa = 2\pi \times 0.1$ MHz. Compared to the ideal case, the interference structure is unchanged but exhibits reduced contrast. Fig. (j)-(l) show the carving process on the atomic ensemble, showing the Dicke state distribution of the initial CSS (red solid bars), and the frequency spectrum of the incident light (dashed black lines).

sidebands at various frequencies ω_n , which coincide with the possible cavity resonance frequencies. The resultant state of the light is expressed as $|\gamma\rangle = \sum_n A_n |\omega_n\rangle$, where A_n is the complex amplitude of frequency component ω_n . When this light is incident onto the cavity, the frequency component ω_n is transmitted through the cavity only when there are n atoms in state $|\uparrow\rangle$. The transmission of other frequency components corresponds to other values of S_z . Thus the strongly coupled atom-cavity system generates correlations between the spectrum of the transmitted light and the possible S_z values of the collective atomic spin. The quantum state of the atom-light system when a single photon has been transmitted is then

$$|\Psi_t\rangle = \sum_{n=0}^{2S} c_n A_n |S, -S + n\rangle \otimes |\omega_n\rangle. \quad (4)$$

Subsequently, we measure the transmitted weak light

with a single-photon detector. If a transmitted photon is detected in the state $|\gamma'\rangle = \sum_n B_n |\omega_n\rangle$, then the collective atomic spin is projected onto

$$|\psi\rangle = C \sum_{n=0}^{2S} A_n B_n^* c_n |S, -S + n\rangle, \quad (5)$$

where C is a normalization factor.

By controlling the amplitude and phase of the coefficients A_n and B_n , we can generate an arbitrary quantum state $|\psi\rangle$ of the atomic spin by simply detecting a single photon in the state $|\gamma'\rangle$. The effect is a carving process on the initial CSS. The cavity transmission in combination with photon detection in state $|\gamma'\rangle$ engraves the coefficients of different Dicke states, and projects the collective atomic spin into a chosen, potentially highly entangled state $|\psi\rangle$. The carving is efficient in that the state generation probability is simply given by the projection $|\langle\theta, \phi|\psi\rangle|^2$ of the initial CSS $|\theta, \phi\rangle$ onto the desired final state $|\psi\rangle$.

We plot a few examples of Schrödinger's cat states carved with this method. In Fig. 2, we display both the Husimi Q function and the Wigner function [36] to characterize the entangled atomic state, where the Q function shows the separation between different quasi-probability regions, and the Wigner function displays the coherence in the form of fringes. Using merely three frequencies, $\omega_k, \omega_{k+p}, \omega_{k+2p}$, we can generate a p -fold symmetric entangled state by projecting the atomic state into different superpositions of $|S, -S + k\rangle, |S, -S + k + p\rangle$ and $|S, -S + k + 2p\rangle$, where k can be an arbitrary integer.

Since a weak incident light beam can be easily prepared as a superposition of frequency components $\sum_n A_n |\omega_n\rangle$ by a combination of frequency and amplitude modulation, the remaining challenge is how to measure the transmitted photon in the $|\gamma'\rangle$ basis. We propose one universal and simple detection scheme which can project the photon into a superposition of different frequencies $|\gamma'\rangle = \sum_n B_n |\omega_n\rangle$.

Let us start with the simplest case. If the incident weak light pulse is monochromatic with frequency ω_n , we simply measure the cavity transmission. (We assume that the pulse is long compared to the cavity decay time κ^{-1} , so that it can be approximated as monochromatic.) If there is a photon detection event, the atomic collective spin is projected into the Dicke state $S_z = -S + n$. This is a useful and fast way to prepare a Dicke state of the atomic ensemble, which is similar to the scheme of Ref. [37], where, however, many photons were used for the detection.

If the input pulse corresponds to a superposition of two frequencies, $|\gamma\rangle = A_n |\omega_n\rangle + A_m |\omega_m\rangle$, we record the transmission time τ of the photon. This situation corresponds to a photon annihilation operator at the detector for time t :

$$\hat{E}^-(t) = A(\hat{a}_{\omega_n} e^{-i\omega_n t} + \hat{a}_{\omega_m} e^{-i\omega_m t}), \quad (6)$$

where A is a constant coefficient, \hat{a}_{ω_i} is the annihilation operator for a photon of frequency ω_i , and we have assumed that the photon detector is sufficiently broadband so that it does not distinguish between the frequency components ω_n, ω_m . For a given detection time τ , there always exist one "bright" photon state $|\gamma_+(\tau)\rangle$ and one "dark" photon state $|\gamma_-(\tau)\rangle$

$$|\gamma_{\pm}(\tau)\rangle = \frac{1}{\sqrt{2}} \left(|\omega_n\rangle \pm e^{i(\omega_m - \omega_n)\tau} |\omega_m\rangle \right), \quad (7)$$

where $\hat{E}^-(\tau)|\gamma_-(\tau)\rangle = 0$. This implies that once we detect a photon at time τ , the photon will be projected onto the bright state $|\gamma_+(\tau)\rangle$. From Eq. 7 in combination with Eq. 5 we see that, for detecting a photon at time τ compared to detecting the photon at time $\tau = 0$, the atomic ensemble gains an additional azimuthal phase of $\Omega\tau$. After photon detection, we can easily apply a spin rotation to the ensemble as a feedforward, correcting for this additional phase according to the detection time τ .

Similar detection and feedback processes also work when the photon has more than two frequency components. If there are p frequency components, we write out the corresponding annihilation operator at time t as

$$\hat{E}^-(t) = A \sum_{j=1}^p \hat{a}_{\omega_{n_j}} e^{-i\omega_{n_j} t}. \quad (8)$$

There is always one bright state,

$$|\gamma_+(\tau)\rangle = \frac{1}{\sqrt{p}} \sum_{j=1}^p e^{i\omega_{n_j} \tau} |\omega_{n_j}\rangle, \quad (9)$$

and $p - 1$ dark states $\{|\gamma_{-j}(\tau)\rangle\}$ for τ , the time that the photon is detected, having $\hat{E}^-(\tau)|\gamma_{-j}(\tau)\rangle = 0$. Upon detecting a photon at time τ , which projects the photon into $|\gamma_+(\tau)\rangle$, we apply a rotation pulse $\Omega\tau$ to correct the phase of the atomic ensemble.

Therefore once a photon with an arbitrary number of frequency components is transmitted through the optical cavity and detected, we can always create the corresponding desired atomic spin state by a rotation applied to all the atoms that is determined by the photon detection time. Note that the average transmitted photon number must be kept much smaller than one, in order to avoid that a second undetected photon changes the atomic spin state.

So far, we have assumed that the cavity lines are perfectly resolved, i.e. that a photon at frequency ω_n is transmitted if and only if the atomic collective spin takes on the value $S_z = -S + n$. This situation corresponds to an infinite cooperativity parameter [38]. In reality, at finite cooperativity, the cavity amplitude transmission function is a Lorentzian of finite width that for n atoms

in $|\uparrow\rangle$ state given by [38]

$$\mathcal{T}(\delta, n) = \frac{1}{1 + \frac{n\eta}{1+4(\Delta+\delta)^2/\Gamma^2} - 2i \left[\frac{\delta}{\kappa} - n\eta \frac{(\Delta+\delta)/\Gamma}{1+4(\Delta+\delta)^2/\Gamma^2} \right]}. \quad (10)$$

Here, $\eta = 4g^2/(\Gamma\kappa)$ is the cavity cooperativity, Γ and κ are the linewidth of the atomic transition and optical cavity, respectively, Δ is the cavity-atom detuning, and δ is the light-cavity detuning. Note that the scattering of photons into free space only decreases the success probability of photon transmission, and slightly reduces the length of the collective spin vector S , but does not otherwise reduce the quality of the final spin state.

So we can write the transmitted state at finite cooperativity as

$$|\Psi_t\rangle = \sum_{n=0}^{2S} c_n |S, -S+n\rangle \sum_k A_k \mathcal{T}(\omega_k - \omega_c, n) |\omega_k\rangle. \quad (11)$$

When we project the photon onto state $\sum_k B_k |\omega_k\rangle$ by photon measurement, the final atomic state becomes

$$|\psi\rangle = C' \sum_{n=0}^{2S} \sum_k A_k B_k^* \mathcal{T}(\omega_k - \omega_c, n) c_n |S, -S+n\rangle, \quad (12)$$

where C' is a normalization factor.

The finite cooperativity thus leads to an admixture of Dicke states neighboring the desired Dicke state, and an imperfect spin state fidelity compared to the desired ideal state. We assume a cavity cooperativity of $\eta = 200$, and set $\Delta = 2\pi \times 66$ MHz, $\Gamma = 2\pi \times 5.2$ MHz, $\kappa = 2\pi \times 0.1$ MHz, which are realistic parameters for Cesium in a high-finesse optical cavity. Compared to the ideal case, the Wigner function looks similar but with a lower contrast than the ideal case, as shown in Fig 2. The finite cooperativity also leads to a nonlinear cavity transmission spectrum. It introduces lower transmission and a broader cavity linewidth for higher-order Dicke state component due to larger absorption by more atoms in the $|\uparrow\rangle$ state. The S_z -dependent transmission reduction can be compensated by adjusting the amplitudes of the frequency components for the input photon. However, the broadening of the cavity lines due to atomic absorption deteriorates the cavity filtering behavior for the Dicke state components, and the admixture of unwanted Dicke states suppresses the fidelity of the generated state compared to the target state. The filtering can be improved by increasing the cavity cooperativity η and choosing a corresponding larger detuning Δ . This is illustrated in Fig. 3, where the fidelity and success probability for various Dicke states, and for a superposition of Dicke states, are shown.

In order to apply this state-carving method for metrology beyond the standard quantum limit, we plot the metrological gain for different Dicke states, for a superposition of Dicke states, as well as for a squeezed state,

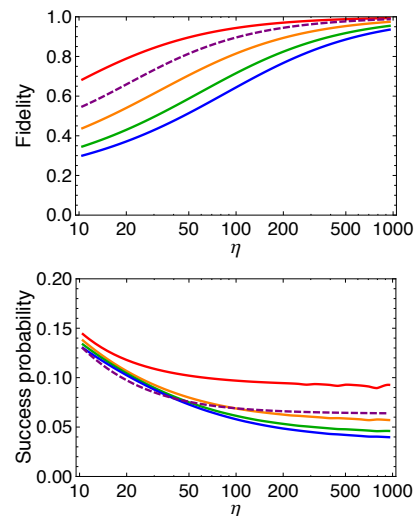


FIG. 3. Fidelity and success probability for generating the Dicke states $S_z = -S + n$ with $n = 1, n = 3, n = 5, n = 7$ (solid lines, top to bottom, red, orange, green and blue), and for an equal superposition of the Dicke states $n = 1$ and $n = 3$ (dashed line). The calculation is for an ensemble of $N = 100$ atoms. For a given cooperativity η , we adjust the cavity-atom detuning and the initial coherent state to maximize the fidelity. The fidelity is monotonically decreasing with n , due to more spin degrees of freedom involved, and the absorptive broadening of the cavity transmission spectrum. Under the same conditions and for the same states, we also plot the success probability for heralding a final state when we send one photon onto the cavity.

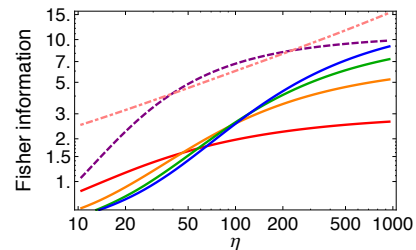


FIG. 4. The metrological gain for Dicke states, a cat state and a squeezed state versus cooperativity η , for $N = 100$ atoms. The solid curves correspond to the Dicke states $S_z = -S + n$ with $n = 1$ (red), $n = 3$ (orange), $n = 5$ (green) and $n = 7$ (blue). The dashed purple line is for an equal superposition of $n = 1$ and $n = 3$. The Fisher information, representing the metrological gain, is normalized to the value for the CSS. The dot-dashed pink line corresponds to the squeezed state generated with single-frequency photon using our scheme. In the latter case, we initiate the atomic ensemble in the coherent state with $\theta = \pi/2$ and $\phi = 0$, and send in a single-frequency pulse $\omega_{N/2}$ which transmits through the cavity at $S_z = 0$. The transmission of the photon squeezes the spin distribution along the S_z direction [5]. The curves show that the created cat state (dashed purple line) is robust at finite η , carrying larger Fisher information than the CSS. At each particular η , we can always carve a cat state such that it has a larger metrological gain than the spin squeezed state generated by a single photon.

as a function of cooperativity η (Fig. 4). The complex states could achieve high metrological gain at a given cooperativity η , as well as display interesting features such as the negative phase-space distribution in Fig. 2.

The cooperativity η can be improved by using advanced techniques, such as micro cavities and higher reflectivity coatings [39]. If we consider the two-component cat state in Fig 2(a) for an ensemble of 100 atoms, the predicted fidelity in the experiment should be 0.63 for $\eta = 20$, 0.88 for $\eta = 100$ and 0.99 for $\eta = 1000$. We have verified that this result does not depend on ensemble size.

In conclusion, we propose a scheme to entangle many atoms by detecting one photon. This universal scheme, that uses only available technology, can efficiently generate a large variety of entangled states. The method resembles a carving process, which engineers the amplitude and phase of each Dicke state, and protects the atomic entanglement from photon scattering loss.

This work was supported by the NSF, DARPA (QUASAR), and MURI grants through AFOSR and ARO. BB acknowledges support from the National Science and Engineering Research Council of Canada. We thank Peter Zoller for discussions and for proposing the term "quantum state carving".

-
- [1] M. Kitagawa and M. Ueda, Phys. Rev. A **47**, 5138 (1993).
 [2] T. Takano, S.-I.-R. Tanaka, R. Namiki, and Y. Takahashi, Phys. Rev. Lett. **104**, 013602 (2010).
 [3] M. H. Schleier-Smith, I. D. Leroux, and V. Vuletić, Phys. Rev. Lett. **104**, 073604 (2010).
 [4] I. D. Leroux, M. H. Schleier-Smith, and V. Vuletić, Phys. Rev. Lett. **104**, 073602 (2010).
 [5] J. G. Bohnet, K. C. Cox, M. A. Norcia, J. M. Weiner, Z. Chen, and J. K. Thompson, Nat Photon **8**, 731 (2014).
 [6] J. Appel, P. J. Windpassinger, D. Oblak, U. B. Hoff, N. Kjrgaard, and E. S. Polzik, Proceedings of the National Academy of Sciences **106**, 10960 (2009).
 [7] I. D. Leroux, M. H. Schleier-Smith, and V. Vuletić, Phys. Rev. Lett. **104**, 250801 (2010).
 [8] M. F. Riedel, P. Bohi, Y. Li, T. W. Hänsch, A. Sinatra, and P. Treutlein, Nature **464**, 1170 (2010).
 [9] C. D. Hamley, C. S. Gerving, T. M. Hoang, E. M. Bookjans, and M. S. Chapman, Nature Physics **8**, 305 (2012).
 [10] C. Gross, T. Zibold, E. Nicklas, J. Estève, and M. K. Oberthaler, Nature **464**, 1165 (2010).
 [11] N. Behbood, G. Colangelo, F. Martin Ciurana, M. Napolitano, R. J. Sewell, and M. W. Mitchell, Phys. Rev. Lett. **111**, 103601 (2013).
 [12] L. M. Duan, M. D. Lukin, J. I. Cirac, and P. Zoller, Nature **414**, 413 (2001).
 [13] H. J. Kimble, Nature **453**, 1023 (2008).
 [14] A. Kuzmich, W. P. Bowen, A. D. Boozer, A. Boca, C. W. Chou, L. M. Duan, and H. J. Kimble, Nature **423**, 731 (2003).
 [15] B. M. Terhal, Rev. Mod. Phys. **87**, 307 (2015).
 [16] L. K. Grover, Phys. Rev. Lett. **85**, 1334 (2000).
 [17] D. Loss and D. P. DiVincenzo, Phys. Rev. A **57**, 120 (1998).
 [18] C. Nayak, S. H. Simon, A. Stern, M. Freedman, and S. Das Sarma, Rev. Mod. Phys. **80**, 1083 (2008).
 [19] L.-M. Duan and H. J. Kimble, Phys. Rev. Lett. **92**, 127902 (2004).
 [20] X.-B. Wang, T. Hiroshima, A. Tomita, and M. Hayashi, Physics Reports **448**, 1 (2007).
 [21] R. McConnell, H. Zhang, J. Hu, S. Čuk, and V. Vuletić, Nature **519**, 439 (2015).
 [22] G. S. Agarwal, P. Lougovski, and H. Walther, Journal of Modern Optics **52**, 1397 (2005).
 [23] D. M. Greenberger, M. A. Horne, A. Shimony, and A. Zeilinger, American Journal of Physics **58**, 1131 (1990).
 [24] D. Leibfried, M. D. Barrett, T. Schaetz, J. Britton, J. Chiaverini, W. M. Itano, J. D. Jost, C. Langer, and D. J. Wineland, Science **304**, 1476 (2004).
 [25] C. F. Roos, M. Riebe, H. Häffner, W. Hänsel, J. Benhelm, G. P. T. Lancaster, C. Becher, F. Schmidt-Kaler, and R. Blatt, Science **304**, 1478 (2004).
 [26] T. Monz, P. Schindler, J. T. Barreiro, M. Chwalla, D. Nigg, W. A. Coish, M. Harlander, W. Hänsel, M. Hennrich, and R. Blatt, Phys. Rev. Lett. **106**, 130506 (2011).
 [27] R. McConnell, H. Zhang, S. Čuk, J. Hu, M. H. Schleier-Smith, and V. Vuletić, Phys. Rev. A **88**, 063802 (2013).
 [28] S. L. Christensen, J.-B. Béguin, E. Bookjans, H. L. Sørensen, J. H. Müller, J. Appel, and E. S. Polzik, Phys. Rev. A **89**, 033801 (2014).
 [29] S. L. Christensen, J. B. Béguin, H. L. Sørensen, E. Bookjans, D. Oblak, J. H. Müller, J. Appel, and E. S. Polzik, New Journal of Physics **15**, 015002 (2013).
 [30] G. Rempe, R. J. Thompson, and H. J. Kimble, Physica Scripta **T51**, 67 (1994).
 [31] R. H. Dicke, Phys. Rev. **93**, 99 (1954).
 [32] T. Vanderbruggen, S. Bernon, A. Bertoldi, A. Landragin, and P. Bouyer, Phys. Rev. A **83**, 013821 (2011).
 [33] E. L. Lehmann and G. Casella, *Theory of Point Estimation (2nd ed.)* (Springer, 1998).
 [34] M. H. Schleier-Smith, I. D. Leroux, and V. Vuletić, Phys. Rev. A **81**, 021804 (2010).
 [35] F. T. Arecchi, E. Courtens, R. Gilmore, and H. Thomas, Phys. Rev. A **6**, 2211 (1972).
 [36] J. P. Dowling, G. S. Agarwal, and W. P. Schleich, Phys. Rev. A **49**, 4101 (1994).
 [37] F. Haas, J. Volz, R. Gehr, J. Reichel, and J. Esteve, Science **344**, 180 (2014).
 [38] H. Tanji-Suzuki, I. D. Leroux, M. H. Schleier-Smith, M. Cetina, A. T. Grier, J. Simon, and V. Vuletić, in *Advances in Atomic, Molecular, and Optical Physics*, Advances In Atomic, Molecular, and Optical Physics, Vol. 60, edited by P. B. E. Arimondo and C. Lin (Academic Press, 2011) pp. 201 – 237.
 [39] D. Hunger, C. Deutsch, R. J. Barbour, R. J. Warburton, and J. Reichel, AIP Advances **2**, 012119 (2012).